First-principles study of vibrational and dielectric properties of β-Si_3N_4

Yongqing Cai, Litong Zhang, Qingfeng Zeng, Laifei Cheng, and Yongdong Xu
National Key Laboratory of Thermostructure Composite Materials, Northwestern Polytechnical University, Xi'an, Shannxi 710072, People's Republic of China

(Received 11 August 2006; published 17 November 2006)

First-principles calculations have been conducted to study the structural, vibrational, and dielectric properties of β-Si_3N_4. Calculations of the zone-center optical-mode frequencies (including longitudinal-optical/transverse-optical splittings), Born effective charge tensors for each atom, and dielectric constants, using density functional perturbation theory, are reported. The fully relaxed structural parameters are found to be in good agreement with experimental data. All optic modes are identified and agreement of theory with experiment is excellent. The static dielectric tensor is decomposed into contributions arising from individual infrared-active phonon modes. It is found that high-frequency modes mainly contribute to the lattice dielectric constant.

DOI: 10.1103/PhysRevB.74.174301 PACS number(s): 63.20.−e, 77.22.−d, 77.84.Bw

Silicon nitride (Si_3N_4) is an industrially important material due to its chemical, mechanical, and electronic properties. Excellent thermomechanical properties have seen this material used for engine parts, bearings, metal machining, and other industrial applications.[1–3] Also, Si_3N_4 is considered to be a promising material for microelectronic applications because of its high dielectric constant and large electronic gap.[4]

Over the past three decades, the lattice dynamical properties of Si_3N_4 have been investigated experimentally as well as theoretically by a number of groups. Brillouin zone center (BZC) phonon frequencies of Si_3N_4 have been measured by using Raman and infrared spectroscopies.[5,6] However, identification of lattice modes in experimental studies is sometimes incomplete, partly because of the complexity of the structure and partly because of experimental errors. Earlier theoretical studies of dynamical properties of Si_3N_4 were done by adopting classical methods.[7,8] Wendel[9] calculated the zone center frequencies through a force field model derived using the Hessian biased technique from *ab initio* calculations. Although good agreement with experimental results for crystal structures, lattice expansion parameters, and the thermodynamical properties was obtained, the accuracy of frequency calculation was limited due to the types of interactions they took into account might not be enough. Recently, first principles calculations of Raman active modes of β-Si_3N_4 have been reported.[10] The calculation was done by using a direct method where the phonon frequencies are calculated from Hellmann-Feynman forces generated by the small atomic displacement.

The first-principles study of phonon frequencies can be performed within a density functional perturbation theory (DFPT) (Ref. 11) or direct method approach.[12] The advantage of the direct method is computationally straightforward and allows one to study phonons in the whole Brillouin zone by perturbing the positions of the atoms slightly and calculating the reaction forces. However, one has to conduct a separate calculation using Berry's phase approach to obtain the longitudinal-optical/transverse-optical (LO-TO) splitting of zone center optical modes. In contrast to the direct method of calculating the phonon frequencies, the linear response approach allows one to obtain the effective charges and dielectric tensors directly with no need to artificially increase the cell size in order to accommodate small values of the **q** vectors as in the direct method approach.

The purpose of this paper is to obtain in more detail the dynamical and dielectric properties of β-Si_3N_4 using the density functional perturbation theory. Our calculations start with the structural optimization and check that our relaxed structural parameters are consistent with the experimental work. The phonon frequencies and Born effective charge tensors are then computed from linear response techniques. Excellent agreement is found between the calculated frequencies and the measured spectra for both IR-active and Raman-active modes. The "missing" A_g mode in Ref. 6 is identified. Finally, the dielectric properties and longitudinal-transverse (LO-TO) mode splittings are investigated, and our theoretical information is combined to predict the lattice contributions to the bulk dielectric tensor. We thus clarify the dependence of the dielectric response on orientation, and lattice dynamical properties and find that high-frequency modes mainly contribute to the lattice dielectric constant.

The calculations are carried using the CASTEP (Refs. 13 and 14) code with norm-conserving pseudopotentials.[15] The $2s$ and $2p$ semicore shells are included in the valence band for N, and the $3s$ and $3p$ are included in the valence band for Si. We employ the Ceperley-Alder[16] local density functional potential as parametrized by Vosko *et al.*[17] The kinetic energy cutoff for the plane waves is 770 eV, Brillouin zone integration is performed using a discrete $4\times4\times10$ Monkhorst-Pack[18] k-point sampling for a primitive cell. The first-principles investigation of vibrational and dielectric properties is conducted within a density functional perturbation theory (DFPT).[11] Phonon frequencies at the zone center, Born effective charge tensors, and dielectric tensor are computed as second-order derivatives of the total energy with respect to an external electric field or to atomic displacements. Technical details can be found in Refs. 19 and 20. To obtain LO/TO splitting characteristic for β-Si_3N_4 we introduced to the dynamical matrix the nonanalytical term proposed by Pick *et al.*[21]

β-Si_3N_4 has a space group $P63/m$. The hexagonal unit cell contains two formula units (14 atoms). Figure 1 shows a ball-stick model of β-Si_3N_4. The silicon nitride structure can be described as a stacking of the idealized Si-N layers in an

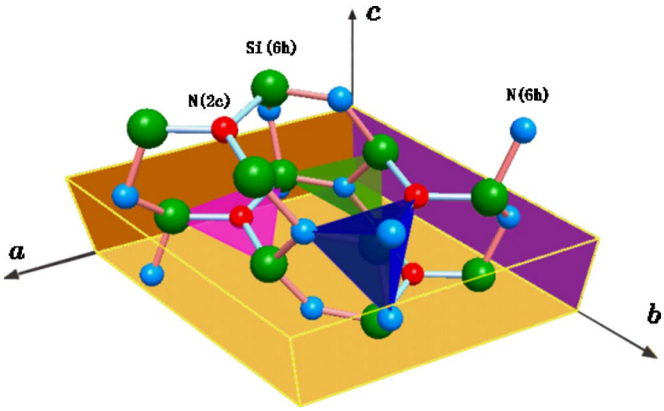

FIG. 1. (Color online) A ball-stick model of β-Si_3N_4. The green (gray), red (dark gray), and blue (light gray) spheres represent Si atoms at 6*h* sites, N atoms at 2*c* sites, N atoms at 6*h* sites, respectively. N atoms are within the same plane of their three nearest neighbors, whereas Si atoms lie at the center of a slightly irregular tetrahedron.

ABAB sequence. All Si atoms are equivalent (6*h* sites), but there are two inequivalent nitrogen sites: N^{2c} at 2*c* sites and N^{6h} at 6*h* sites. The N^{2c} atoms are in a planar geometry with their three Si nearest neighbors, and the N^{6h} atoms are in slightly puckered sites surrounded by three Si atoms, whereas Si atoms are at the center of slightly irregular tetrahedron bonded with one N^{2c} atom and three N^{6h} atoms.

The structural optimization was done by relaxing both the internal coordinates and the lattice constants by calculating the *ab initio* forces on the ions, within the Born-Oppenheimer approximation, until the absolute values of the forces were converged to less than 0.01 eV/Å. The relaxed lattice and fractional internal parameters of the equilibrium structure are listed in Table I and the initial configuration is taken from Ref. 23. It can readily be seen that there is excellent agreement between our results and previous experiment. The volumes are slightly underestimated, by 2-3%, as is typical of local density approximation (LDA) calculations. It

TABLE I. Optimized geometry of β-Si_3N_4 ($P63/m$)

Parameter	Experiment[a]	Experiment[b]	This work
V (Å^3)	147.016	145.881	142.700
c (Å)	7.6272	7.6070	7.5572
a (Å)	2.9182	2.9110	2.8852
xSi (6*h*)	0.1842	0.1740	0.1742
ySi (6*h*)	0.7704	0.7660	0.7678
zSi (6*h*)	0.2500	0.2500	0.2500
xN (2*c*)	0.3333	0.3333	0.3333
yN (2*c*)	0.6667	0.6667	0.6667
zN (2*c*)	0.2500	0.2500	0.2500
xN (6*h*)	0.3399	0.3210	0.3302
yN (6*h*)	0.0357	0.0250	0.0299
zN (6*h*)	0.2500	0.2500	0.2500

[a]Reference 22.
[b]Reference 23.

TABLE II. Zone center optic phonon frequencies of β-Si_3N_4 (cm^{-1})

Mode	Experiment[a] (144 A_g)	Experiment[b] (145 A_g)	Theory[c]	Theory[d]	This work
Raman					
E_{2g}	186	185	183	190	181
A_g	210	208	201	236	200
E_{1g}	229	230	228	215	225
E_{2g}	451	452	444	518	444
A_g	···	···	457	289	456
E_{2g}	619	620	603	592	610
A_g	732	733	715	539	725
E_{1g}	865	866	836	975	859
E_{1g}	928	930	897	1017	921
A_g	939	940	908	547	930
E_{2g}	1047	1048	1012	1067	1035
Infrared					
A_u	380				378
E_{2u}	447				424
E_{2u}	580				562
A_u	910				848
E_{2u}	985				886
E_{2u}	1040				1021

[a]Reference 5.
[b]Reference 6.
[c]Reference 10.
[d]Reference 9.

should be noted that the accuracy in comparison with experimental lattice constants is much lower for two reasons: (a) DFT in the LDA is an approximation to the exact n-electron problem. (b) Temperature effects are neglected in the calculations; the calculations are performed for a fictitious classical system at zero temperature.

Since the primitive unit cell of β-Si_3N_4 structure has 14 atoms, there are a total of 42 modes of vibration. The irreducible representation at the center of the Brillouin zone is

$$\Gamma_{optic} = 4A_g(R) + 2E_{1g}(R) + 5E_{2g}(R) + 2A_u(IR) + 4E_{1u}(IR) + 3B_g + 2E_{2u},$$

$$\Gamma_{acoustic} = A_u + E_{1u}.$$

Because of inversion symmetry, IR and Raman modes are mutually exclusive.

In Table II, we compare calculated phonon frequencies at the Γ point with the measured Raman[5,6] and infrared[5] values. For comparison, we cite also the phonon frequencies from theoretical calculations through direct methods[10] and classical model.[9] Our calculated Raman active mode frequencies present a rms absolute deviation of 8.6 cm^{-1}, and a rms relative deviation of 1.9% with respect to the measurements of Ref. 6. This is an excellent agreement with both experiments and theory, and makes us very confident in the prediction of the frequencies for the IR active modes. It should be noted

TABLE III. LO/TO splittings for infrared active modes of β-Si_3N_4. The first column ($E=0$) is for no electric field, the second is for the field lying in the plane ($E\|a-b$), and the third is for $E\|c$. $\Delta\omega^2=\omega_{LO}^2-\omega_{TO}^2$.

	Phonon frequency (cm^{-1})			
Mode	$E=0$	$E\|a-b$	$E\|c$	$\sqrt{\Delta\omega^2}(cm^{-1})$
A_u	378	378	395	115
E_{2u}	424	453	424	159
E_{2u}	562	584	562	159
A_u	848	848	1056	629
E_{2u}	886	1026	886	517
E_{2u}	1021	1150	1021	529

that the values of the vibrational properties of β-Si_3N_4 through the empirical model proposed by Wendel are just qualitative. Because of weak intensity and closeness to a relatively stronger E_{2g} mode, the A_g mode in the intermediate frequency band was misidentified[5,6] and is now known to be 457 cm^{-1} through theoretical calculation.[10] Our calculation shows that this mode is at 456 cm^{-1}, which is in very good agreement with previous theoretical calculations.

The IR modes group into modes with displacements either in the x,y plane or along the z direction. The E_{1u} mode has displacement pattern in the x,y plane, and the A_u mode has displacements along z. For IR active mode, the root mean square relative deviation of our results with experimental data is 4.9%, with a slight overall tendency to underestimation. For some of the modes, there are large differences with the reported experimental frequencies.[5] For example, our calculated frequency for the E_{2u} mode is 886 cm^{-1}, whereas the experimental value is 985 cm^{-1}; the origin of these discrepancies is unclear. The LO/TO splittings for the infrared active mode are presented in Table III. The LO/TO splittings for displacements parallel to the layers occur for the E_{2u} mode and displacements parallel to c principal axis occur for the A_u mode. The large LO/TO splittings of the three highest modes suggest they involve large effective charges and make large contributions to the static dielectric tensor of β-Si_3N_4.

The Born effective charge tensor quantifies the macroscopic electric response of a crystal to the internal displacements of its atoms. Our results for the dynamical effective charges of β-Si_3N_4 are presented in Table IV for atoms at the $6h$ Wyckoff sites in the $z=0.75$ plane and two nitrogen atoms at $2c$ sites. The effective charges for the other atoms can be obtained from those shown in the table by symmetry considerations.

TABLE IV. The Born effective charges of β-Si_3N_4. $Z_j^*(j=1,2,3)$ is the jth eigenvalue of the symmetric part of the Z^* tensor. $\bar{Z}$ is the average of eigenvalues. Only atoms at the $6h$ Wyckoff sites in the $z=0.75$ plane are presented.

	N_1^{2c}	N_2^{2c}	N_1^{6h}	N_2^{6h}	N_3^{6h}	Si_1^{6h}	Si_2^{6h}	Si_3^{6h}
Z_1^*	−2.95	−2.95	−1.61	−3.15	−1.61	3.15	3.58	3.15
Z_2^*	−2.95	−2.95	−3.15	−1.61	−3.15	3.58	3.15	3.58
Z_3^*	−1.76	−1.76	−2.82	−2.82	−2.82	3.41	3.41	3.41
$\bar{Z}$	−2.55	−2.55	−2.53	−2.53	−2.53	3.38	3.38	3.38

It is obvious that both Si and N atoms have lower effective charges than their formal charges,+4 and −3 for Si and N respectively, relating to the covalency of Si-N bonds. The Si atoms tend to show a more isotropic character than N atoms. As discussed above, the nitrogen atoms at the $2c$ sites are bonded to three nearest-neighbor silicon atoms in a planar configuration. One might then expect that the largest dynamical charge transfer would occur for motions of the N atoms in this plane. To check this, we computed the eigenvalues in the second column of Table IV. Sure enough, the principal axis associated with the eigenvalue $Z_3^*=-1.76$ of the smallest magnitude points normal to the plane of the neighbors. The other two principle axes lie in the plane of the neighbors. Not surprisingly in view of its tetrahedral coordination, the Z^* tensor for atom Si is more isotropic, as indicated by the smaller spread of the eigenvalues in the table.

Crystal symmetry makes the dielectric tensors be composed of some independent components. In hexagonal symmetry such as β-Si_3N_4, the calculated electronic (ε_∞) and static (ε_0) dielectric tensors are diagonal and have two independent components $\varepsilon_\perp$ and $\varepsilon_\|$ perpendicular to and along the c axis, respectively. The electronic dielectric constants are calculated to be $\varepsilon_\perp^\infty=4.19$ and $\varepsilon_\|^\infty=4.26$. The reported value of ε^∞ is 4.0 (Ref. 24), and our theoretical values tend to be overestimated in local density approximation (LDA) calculations due to the underestimation of the band gap.[25]

According to the generalized Lyddane-Sachs-Teller (LST) relation,[26]

$$\varepsilon_0=\varepsilon_\infty\prod_m\frac{\omega_{LO,m}^2}{\omega_{TO,m}^2}, \tag{1}$$

which is used separately for each polarization; the static dielectric constants ε_0 of both directions are $\varepsilon_\perp^0=8.79$ and $\varepsilon_\|^0=7.21$ respectively, showing nearly isotropic character. The dielectric properties of crystalline Si_3N_4 have not been studied very much experimentally. Experimental reports of the value of ε_0 for polycrystalline Si_3N_4 span a wide range from about 8.1 to 8.6 (Ref. 27), our orientationally average static dielectric constant is 8.26, falling comfortably in this range.

The static dielectric tensor ε_0 can also be separated into contributions arising from purely electronic screening ε^∞ and IR-active phonon modes according to[20]

$$\varepsilon_0=\varepsilon_\infty+\frac{4\pi}{V_0}\sum_m\frac{S_m}{\omega_{TO,m}^2}=\varepsilon_\infty+\varepsilon_\infty\sum_m\frac{\omega_{LO,m}^2-\omega_{TO,m}^2}{\omega_{TO,m}^2}, \tag{2}$$

where V_0 denotes the volume of the primitive unit cell. The derivation of Eq. (2) follows from the relation[20] between the mode oscillator strength S_m and the corresponding LO-TO splitting, whereas Eq. (1) is obtained based on the adiabatic, electrostatic, and harmonic approximation. The contributions to the static dielectric tensor can be examined mode by mode through Eq. (2). The differences between Eq. (1) and Eq. (2) are small, however. The static dielectric constants of both directions from Eq. (2) are $\varepsilon_\perp^0=7.67$ and $\varepsilon_\|^0=6.99$, compared to that of $\varepsilon_\perp^0=8.79$ and $\varepsilon_\|^0=7.21$ from Eq. (1). For IR-active

TABLE V. IR active mode frequency, contribution to the component of dielectric tensor for each IR-active mode. The component of lattice dielectric constant parallel (perpendicular) to the c axis is denoted $\varepsilon_{\parallel}^{lat}$ ($\varepsilon_{\perp}^{lat}$).

Mode	ω_{TO} (cm^{-1})	ω_{LO} (cm^{-1})	$\sqrt{\Delta\omega^2}$ (cm^{-1})	$\varepsilon_{\perp}^{lat}$	$\varepsilon_{\parallel}^{lat}$
A_u	378	395	115	0	0.39
E_{2u}	424	453	159	0.59	0
E_{2u}	562	584	159	0.34	0
A_u	848	1056	629	0	2.34
E_{2u}	886	1026	517	1.43	0
E_{2u}	1021	1150	529	1.12	0

modes, the mode frequencies and contributions to the dielectric tensor are displayed in Table V. It can be seen that the high-frequency modes mainly contribute to the lattice dielectric constant. Although the mode contribution to the static dielectric constant is inversely proportional to the square of the mode frequency [Eq. (2)], low frequency modes A_u at 378 cm^{-1}, E_{2u} at 424 and 562 cm^{-1} make relatively small contributions to the static dielectric tensor due to their smaller LO/TO splittings compared to higher frequency modes. When all the modes are summed over, we obtain the total lattice dielectric components of β-Si_3N_4 are $\varepsilon_{\perp}^{lat}=3.48$ and $\varepsilon_{\parallel}^{lat}=2.73$ compared to electronic contributions of $\varepsilon_{\perp}^{\infty}=4.19$ and $\varepsilon_{\parallel}^{\infty}=4.26$. We can conclude that β-Si_3N_4 has a lattice dielectric constant smaller than that of the electronic contribution.

In conclusion, we have used density functional perturbation theory (DFPT) to investigate the vibrational and dielectric properties of β-Si_3N_4. Firstly, the structural parameters, including the internal coordinates, are relaxed, and excellent agreement is achieved with experimental results. The vibrational modes at the center of the Brillouin zone have been evaluated and compared with experiment. All modes are identified and compared with experiments and previous theoretical calculations. The calculated zone-center phonon mode frequencies are in good agreement with infrared and Raman experiments. Finally, The Born effective charge tensors, and the dielectric permittivity tensors have also been calculated. The mode contributions to the dielectric tensors have been obtained. We find that β-Si_3N_4 has a lattice dielectric constant smaller than that of electronic contribution.

The authors acknowledge support from the Natural Science Foundation of China (Contract No. 90405015), from the National Young Elitists Foundation (Contract No. 50425208) and from the Program for Changjiang Scholars and Innovative Research Team in university (PCSIRT). We thank Northwestern Polytechnical University High Performance Computing Center for allocation of computing time on their machines.

[1] F. de Brito Mota, J. F. Justo, and A. Fazzio, Phys. Rev. B **58**, 8323 (1998).
[2] F. L. Riley, J. Am. Ceram. Soc. **83**, 245 (2000).
[3] R. N. Katz, Science **208**, 84 (1980).
[4] M. J. Powell, B. C. Easton, and O. F. Hill, Appl. Phys. Lett. **38**, 794 (1981).
[5] N. Wada, S. A. Solin, J. Wong, and S. Prochazka, J. Non-Cryst. Solids **43**, 7 (1981).
[6] K. Honda, S. Yokoyama, and S. Tanaka, J. Appl. Phys. **85**, 7380 (1999).
[7] C. M. Marian, M. Gastreich, and J. D. Gale, Phys. Rev. B **62**, 3117 (2000).
[8] M. Gastreich, J. D. Gale, and C. M. Marian, Phys. Rev. B **68**, 094110 (2003).
[9] J. A. Wendel and W. A. Goddard III, J. Chem. Phys. **97**, 5048 (1992).
[10] J. Dong and O. F. Sankey, J. Appl. Phys. **87**, 958 (2000).
[11] S. Baroni, S. de Gironcoli, A. Dal Corso, and P. Giannozzi, Rev. Mod. Phys. **73**, 515 (2001).
[12] G. J. Ackland, M. C. Warren, and S. J. Clark, J. Phys.: Condens. Matter **9**, 7861 (1997).
[13] M. D. Segall, P. J. D. Lindan, M. J. Probert, C. J. Pickard, P. J. Hasnip, S. J. Clark, and M. C. Payne, J. Phys.: Condens. Matter **14**, 2717 (2002).
[14] G. J. Ackland, M. C. Warren, and S. J. Clark, J. Phys.: Condens. Matter **9**, 7861 (1997).
[15] D. R. Hamann, M. Schlüter, and C. Chiang, Phys. Rev. Lett. **43**, 1494 (1979).
[16] D. M. Ceperley and B. J. Alder, Phys. Rev. Lett. **45**, 566 (1980).
[17] S. H. Vosko, L. Wilk and M. Nusair, Can. J. Phys. **58**, 1200 (1980).
[18] H. J. Monkhorst and J. D. Pack, Phys. Rev. B **13**, 5188 (1976).
[19] X. Gonze, Phys. Rev. B **55**, 10 337 (1997).
[20] X. Gonze and C. Lee, Phys. Rev. B **55**, 10 355 (1997).
[21] R. Pick, M. H. Kohen, and R. M. Martin, Phys. Rev. B **1**, 910 (1970).
[22] M. Billy, J.-C. Labbe, A. Selvaraj, and G. Roult, Mater. Res. Bull. **18**, 921 (1983).
[23] O. Borgen and H. M. Seip, Acta Chem. Scand. (1947-1973) **15**, 1789 (1961).
[24] S. K. Andersson, Ö. Staaf, P. O. Olsson, A. Malmport, and C. G. Ribbing, Opt. Mater. **10**, 85 (1998).
[25] Ph. Ghosez, J.-P. Michenaud, and X. Gonze, Phys. Rev. B **58**, 6224 (1998).
[26] W. Cochran and R. A. Cowley, J. Phys. Chem. Solids **23**, 447 (1962).
[27] M. K. Park, H. N. Kim, K. S. Lee, S. S. Baek, E. S. Kang, Y. K. Baek, and D. K. Kim, Key Eng. Mater. **287**, 247 (2005).